



HAL
open science

Improved VSF algorithm for smooth surface reconstruction from sparse medical data

Ahmad Almhdie, Christophe Léger, Maïtine Bergounioux, Mohamed Deriche,
Roger Lédée

► **To cite this version:**

Ahmad Almhdie, Christophe Léger, Maïtine Bergounioux, Mohamed Deriche, Roger Lédée. Improved VSF algorithm for smooth surface reconstruction from sparse medical data. *Journal of Computing and Information Technology*, 2007, 15 (2), pp.123-130. 10.2498/cit.1000820 . hal-00607885

HAL Id: hal-00607885

<https://hal.science/hal-00607885>

Submitted on 11 Jul 2011

HAL is a multi-disciplinary open access archive for the deposit and dissemination of scientific research documents, whether they are published or not. The documents may come from teaching and research institutions in France or abroad, or from public or private research centers.

L'archive ouverte pluridisciplinaire **HAL**, est destinée au dépôt et à la diffusion de documents scientifiques de niveau recherche, publiés ou non, émanant des établissements d'enseignement et de recherche français ou étrangers, des laboratoires publics ou privés.

Improved VSF Algorithm for Smooth Surface Reconstruction from Sparse Medical Data

Ahmad Almhdie^{1,4}, Christophe Léger¹, Maïtine Bergounioux²,
Mohamed Deriche³ and Roger Lédée¹

¹LESI, Polytech'Orléans, Université d'Orléans, Orléans, France

²MAPMO, Faculté des Sciences, Université d'Orléans, France

³Electrical Engineering Department, King Fahd University of Petroleum and Minerals, Saudi Arabia

⁴Electrical and Communication Engineering Department, University of Sebha, Libya

This paper presents a Modified Variational Splines Fitting (MVSF) algorithm for surface reconstruction using thin plate splines on scattered patches or points of originally smooth surfaces. In particular, a more accurate derivation of the discrete equations for the energy corresponding to the thin plate model is introduced. The results obtained on simulated data show that the proposed algorithm converges faster than the original VSF algorithm. Additionally, we discuss an approach for choosing the algorithm's parameters using a cross validation technique. Results obtained with the modified algorithm are compared to those using a Frequency Fourier-based 3D Harmonic modelling (3DHM) algorithm and show that the proposed algorithm gives an improved performance under the small sample size condition. The developed model has been successfully applied for real biomedical data; in particular for the reconstruction of left ventricle of human heart.

Keywords: sparse or scattered data, medical data, surface reconstruction, thin plate model, smooth surface

1. Introduction

Surface reconstruction and smoothing methods are widely used in practice to best estimate the original surface represented by a scattered noisy point set arising in a number of scientific and engineering application domains including medical imaging applications [1]. For instance, the number and the distribution of the initial samples of an organ surface lead to incomplete meshes. Stacks of two-dimensional contours can also be used to reconstruct three-dimensional surfaces [2]. The problem of surface reconstruction can be solved using a variety

of techniques. The finite element method is one of these techniques. An example of this method is the use of Voronoi diagram and Delaunay triangulation [3] to find the topological connection of the sample points.

Another type of reconstructing smooth surfaces rely on the finite difference methods using deformable models [4] such as thin plate model [5]. The main idea is to create an initial mesh and deform it to best match the range input data. This is usually expressed as an energy minimisation problem. There are two forces that formulize the final shape of the reconstructed surface. One attracts the surface towards the input data and the other tries to keep the surface smooth. Fourier-based interpolation methods [6], to mention a few, are also used in the domain of surface reconstruction. These methods are generally computationally inexpensive, but comparably more sensitive to number of missing points. The former two approaches were selected for further study in this work as these are generally more appropriate for smooth surfaces such as surfaces of left ventricle of heart. In general, methods based on deformable models give nice smooth surfaces, but are computationally expensive and complex. We present in this work a faster and less complex algorithm compared to a previous algorithm proposed by Richard Szeliski. The rest of this paper is organized as follows: in Section 2, both spline-based and frequency-based algorithms are described. In Subsection 2.1, an introduction to variational splines fitting algorithms is given. The data

compatibility constraint of the thin plate model and the smoothness constraint are also presented in this section. We then introduce our modification to the original VSF algorithm in order to improve its performance. The resulting algorithm is called the Modified Variational Splines Fitting (MVSF) algorithm. At the end of the section, the overall discrete optimization problem is formulated. For comparison reasons, the Fourier-based 3DHM algorithm is described in Subsection 2.2. This algorithm was previously developed by the authors. Simulation results are presented in Section 3 and application results are presented in Section 4. We finally conclude our paper in Section 5 by a summary and some keynotes for future work.

2. Algorithm Description

2.1. Variational Splines Fitting Algorithms

In [7], Szeliski proposed to use a deformable model to estimate the missing points (here we call it VSF). In this algorithm, the problem is formulated as an optimization one. The function to be minimized is written:

$$E(x) = E_d(x) + \lambda E_s(x), \quad (1)$$

where

$$x = [x_{i,j}], \quad (i = 0 : N - 1, j = 0 : M - 1)$$

are the mesh regular points of the reconstructed surface, i and j indicate spatial positions. This function includes two constraints: the data compatibility constraint $E_d(x)$, and the smoothness constraint $E_s(x)$. λ ($\lambda > 0$) is the regularization parameter which is used to adjust the closeness of the fit between the surface and the sparse data set. This parameter depends on the sparse data set and can be estimated using a generalised cross validation technique. In general, as λ increases, the reconstructed surface becomes smoother. However, the probability of error between the original sparse samples and their corresponding estimated ones becomes higher. For very high values of λ , ($\lambda \approx \infty$), the fitted surface tends towards a flat one. As λ tends to zero, this probability becomes smaller, but the reconstructed surfaces might no longer be smooth.

The above formulation is usually expressed as an energy minimisation problem where an attracting force draws the mesh towards the sparse

data and a tension in the mesh keeps the surface smooth [2].

The data compatibility constraint measures the distance between the original sparse points and the interpolated smooth surface. The energy expression corresponding to the data compatibility constraint can be written as:

$$\varepsilon_d(x) = \frac{1}{2} \sum_i w_i (f(u_i, v_i) - d_i)^2. \quad (2)$$

The discrete form is:

$$E_d(\mathbf{x}, \mathbf{d}) = \frac{1}{2} \sum_{i,j} \mathbf{w}_{i,j} (\mathbf{x}_{i,j} - \mathbf{d}_{i,j})^2, \quad (3)$$

where $x_{i,j}$ stands for the discrete values of $f(u_i, v_i)$: $\mathbf{x}_{i,j} = f(u_i, v_i)$, $\mathbf{d}_{i,j}$ ($\mathbf{d}_{i,j} = 0$ at missing points) are the sparse samples of the original incomplete surface and the weights $w_{i,j}$ ($w_{i,j} = 0$ at missing points) are inversely related to the variance of the measurements. The higher the weights, the better the reconstructed surface fits the original sparse samples. In this case, the data compatibility constraint overinfluences the overall energy function and the reconstructed surface become no longer smooth.

Reassembling all mesh points into a vector \mathbf{x} , one can rewrite equations (3) in a matrix form. The energy corresponding to the data compatibility constraint becomes:

$$E_d(\mathbf{x}, \mathbf{d}) = \frac{1}{2} (\mathbf{x} - \mathbf{d})^T \mathbf{A}_d (\mathbf{x} - \mathbf{d}), \quad (4)$$

where \mathbf{d} is a zero-padded vector of data values and the diagonal matrix \mathbf{A}_d has entries w_i at which the data coincide with the sparse data points and zeros elsewhere. In particular, this allows treating problems with missing or unknown data.

Using the thin plate model, the energy function corresponding to the smoothness constraint can be written in continuous form as:

$$\varepsilon_s(f) = \frac{1}{2} \int \int (f_{uu}^2 + f_{vv}^2 + 2f_{uv}^2) \, dudv, \quad (5)$$

where $f : f(u, v)$ is the smoothed continuous functional of the interpolated surface in u and v directions; and the subscripts uu , vv and uv indicate partial derivatives.

Original VSF Algorithm

In the original VSF algorithm, the discrete form of the above energy function is derived using a classical finite-difference scheme. The resulting discrete function is:

$$E_s(x) = \frac{h_u h_v}{2} \sum_{i,j} \left[\left(\frac{\mathbf{x}_{i+1,j} - 2\mathbf{x}_{i,j} + \mathbf{x}_{i-1,j}}{h_u^2} \right)^2 + \left(\frac{\mathbf{x}_{i,j+1} - 2\mathbf{x}_{i,j} + \mathbf{x}_{i,j-1}}{h_v^2} \right)^2 + 2 \left(\frac{\mathbf{x}_{i+1,j+1} - \mathbf{x}_{i,j+1} - \mathbf{x}_{i+1,j} + \mathbf{x}_{i,j}}{h_u h_v} \right)^2 \right], \quad (6)$$

where $h_u = |\Delta u|$ and $h_v = |\Delta v|$ are the step sizes of the regular mesh of the reconstructed surface in the u and v directions respectively.

MVSF Algorithm

In this work, we propose a more accurate derivation process to get the discrete energy corresponding to the above continuous function (5). In particular, we propose to take into consideration higher element components of the corresponding two-variable Taylor formula:

$$E_s(x) = \frac{h_u h_v}{2} \sum_{i,j} \left[\left(\frac{\mathbf{x}_{i+1,j} - 2\mathbf{x}_{i,j} + \mathbf{x}_{i-1,j}}{h_u^2} \right)^2 + \left(\frac{\mathbf{x}_{i,j+1} - 2\mathbf{x}_{i,j} + \mathbf{x}_{i,j-1}}{h_v^2} \right)^2 + \frac{1}{8} \left(\frac{\mathbf{x}_{i+1,j+1} - \mathbf{x}_{i+1,j-1} - \mathbf{x}_{i-1,j+1} + \mathbf{x}_{i-1,j-1}}{h_u h_v} \right)^2 \right]. \quad (7)$$

We can see from the above expression that the first two terms are similar to the original formulation given in equation (6). They both use the so-called 5-star-points scheme.

The main advantage of the expression given in equation (7) is its accuracy in using the 4 diagonal points to approximate the crossed second-order derivative at position (i,j) , as shown in Figure 1. Obviously, Szeliski's approximation is a biased forward approximation, as shown in Figure 2.

Reassembling all mesh points into a vector \mathbf{x} , we can rewrite equations (6) and (7) in a matrix form. The energy corresponding to the thin plate model can also be written in compact form as:

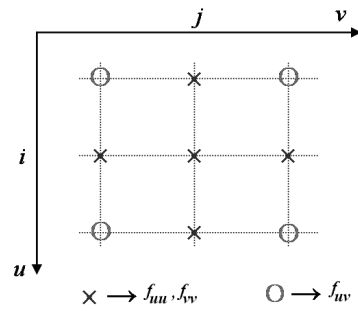


Figure 1. Point estimation using MVSF algorithm.

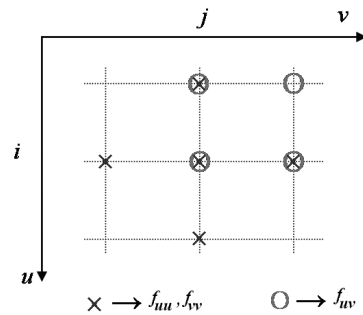


Figure 2. Point estimation using VSF algorithm.

$$E(\mathbf{x}) = \frac{1}{2} \mathbf{x}^T \mathbf{A}_s \mathbf{x}, \quad (8)$$

where the *stiffness* matrix \mathbf{A}_s is a sparse block diagonal matrix. The matrix \mathbf{A}_s has at most 13 non-zero entries per row, as discussed in [7]. The rows with the maximum number of entries are: $(n+1)M + (m+2)$; $n = 1 : N-4$ and $m = 1 : M-4$; N and $M > 4$.

However, when periodicity is imposed upon the *stiffness* matrix \mathbf{A}_s , all rows would then have 13 non-zero entries. Note that such periodicity constraint is appropriate when considering spherical coordinates used in describing human organs. The resulting *stiffness* matrix has a homogeneous structure and can be easily coded.

$$\mathbf{A}_s = \begin{pmatrix} \mathbf{B} & \mathbf{C} & \mathbf{D} & \mathbf{0} & \dots & \mathbf{0} & \mathbf{D} & \mathbf{C} \\ \mathbf{C} & \mathbf{B} & \mathbf{C} & \mathbf{D} & \mathbf{0} & \dots & \mathbf{0} & \mathbf{D} \\ \mathbf{D} & \mathbf{C} & \mathbf{B} & \mathbf{C} & \mathbf{D} & \mathbf{0} & \dots & \mathbf{0} \\ \mathbf{0} & \mathbf{D} & \mathbf{C} & \mathbf{B} & \mathbf{C} & \mathbf{D} & \mathbf{0} & \dots \\ \vdots & \vdots & \vdots & \vdots & \vdots & \vdots & \vdots & \vdots \\ \mathbf{0} & \dots & \mathbf{0} & \mathbf{D} & \mathbf{C} & \mathbf{B} & \mathbf{C} & \mathbf{D} \\ \mathbf{D} & \mathbf{0} & \dots & \mathbf{0} & \mathbf{D} & \mathbf{C} & \mathbf{B} & \mathbf{C} \\ \mathbf{C} & \mathbf{D} & \mathbf{0} & \dots & \mathbf{0} & \mathbf{D} & \mathbf{C} & \mathbf{B} \end{pmatrix}, \quad (9)$$

where \mathbf{B} , \mathbf{C} and \mathbf{D} are $M \times N$ matrices. $\mathbf{0}$ is an $M \times N$ zero matrix.

The Discrete Problem

The combined discrete energy expression can hence be written in matrix form as:

$$E(\mathbf{x}) = \frac{1}{2} \mathbf{x}^T \mathbf{A} \mathbf{x} - \mathbf{x}^T \mathbf{b} + c, \quad (10)$$

where $\mathbf{A} = \lambda \cdot \mathbf{A}_s + \mathbf{A}_d$, $\mathbf{b} = \mathbf{A}_d \cdot \mathbf{d}$ and c is a constant that may be omitted in the minimization process. This energy function has a minimum at $\mathbf{x} = \mathbf{x}^*$, which is the solution of the following linear system that is obtained via the Euler equation:

$$\mathbf{A} \mathbf{x}^* = \mathbf{b}, \quad (11)$$

since \mathbf{A} is a strictly positive matrix. The above set of linear equations is, hence, a high dimension homogeneous positive definite system, that can be solved using the conjugate gradient method, thanks to the strict positivity of the matrix \mathbf{A} .

Our approximation is found to lead to better performance compared to that used in original VSF algorithm.

2.2. 3DHM Fourier-based Algorithm

For comparison purposes, we considered the use of the 3D Harmonic Modelling (3DHM) algorithm (developed previously by the authors [6]). This algorithm is much less complex than the previous thin plate splines algorithm. The 3DHM algorithm reconstructs the incomplete surface using an iterative algorithm based on Fourier analysis. This algorithm consists of four major steps (per iteration):

- A) The 2D Fourier transform $\mathbf{D}(u, v)$ of the k^{th} doubly periodic mesh $x_{i,j}^k$ is computed.
- B) The resulting $\mathbf{D}(u, v)$ is low-pass filtered to reduce discontinuities in the space domain.
- C) The missing points are then estimated using the inverse Fourier transform.
- D) The algorithm terminates the iterations when the Mean Square Error between the estimated values of the missing points from successive iterations falls below a preset threshold ζ . If not, the algorithm restarts using the recently generated mesh ($k = k + 1$) as an input to step A. The data from the initial sparse mesh is retained.

The mean square error (MSE) between successive surfaces is calculated as follows:

$$\frac{1}{N \cdot M} \sum_{i=0}^N \sum_{j=0}^M \left[\mathbf{x}_{i,j}^k - \mathbf{x}_{i,j}^{k+1} \right]^2, \quad (12)$$

where N and M represent the size of the regular mesh in the i^{th} and j^{th} directions, respectively.

3. Simulation Result

Our first aim was to compare the convergence characteristics of the original and modified Szeliski algorithm for relatively smooth surfaces. We then compared the performance of the modified algorithm and that of the 3DHM algorithm. In order to limit the scope of the problem, we adopted the following methodology for choosing the optimal values for the control parameters (ω, λ) .

- A) Choose a smooth surface as a reference model.
- B) Randomly select about 30% of the total surface patches.
- C) Reconstruct the surface using these selected patches.
- D) Calculate the mean square error between the reconstructed surface and the reference model using different values of (ω, λ) .

Figure 3 presents a reference model of a 32×32 smooth surface, and Figure 4 shows a surface with about 70% of missing points. Figure 5 shows a reconstructed surface and Figure 6 shows the main square error between the reference and reconstructed surfaces.

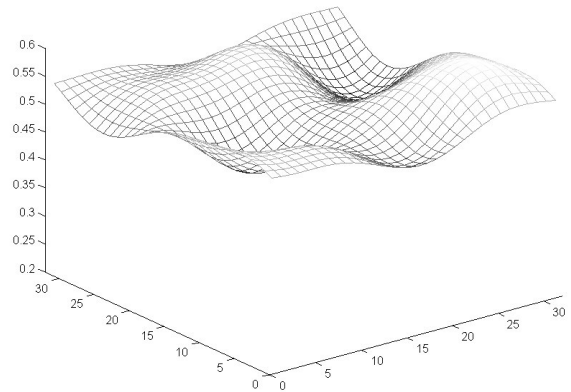


Figure 3. Typical 32×32 smooth surface.

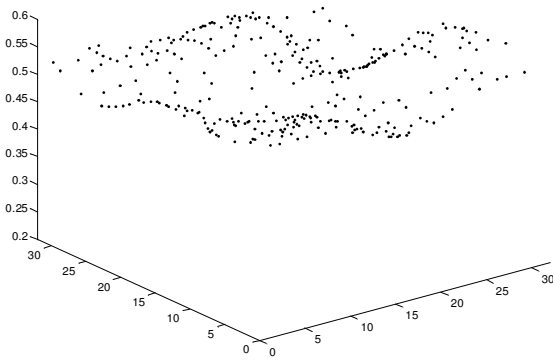


Figure 4. Randomly selected 30% of the total samples of the reference surface.

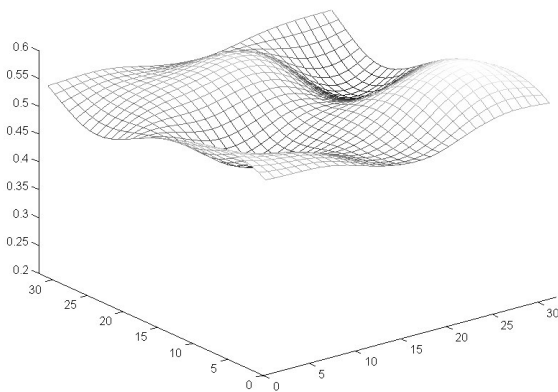


Figure 5. Reconstructed surface.

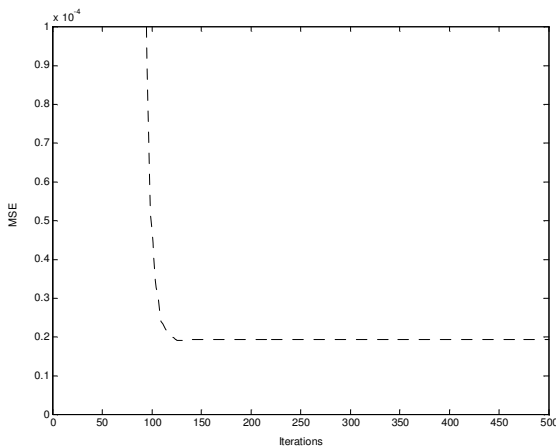


Figure 6. Mean square error between reference and reconstructed surfaces.

Figure 7 displays the MSE as a function of (ω, λ) . Notice that the MSE almost stabilizes when ω is greater than 300 and λ is less than 30. $\omega=314$ is actually the inverse of the variance of the selected sample [7]. The results displayed in Figure 8 show that the proposed algorithm,

MVSF, outperforms the original VSF algorithm, e.g. when the tolerance value of the iterative conjugate gradient algorithm is set to 10^{-4} , the modified algorithm converges about 100 iterations faster than the original algorithm. One can also notice that the inappropriate choice of ω and λ can lead to substantial deterioration in performance.

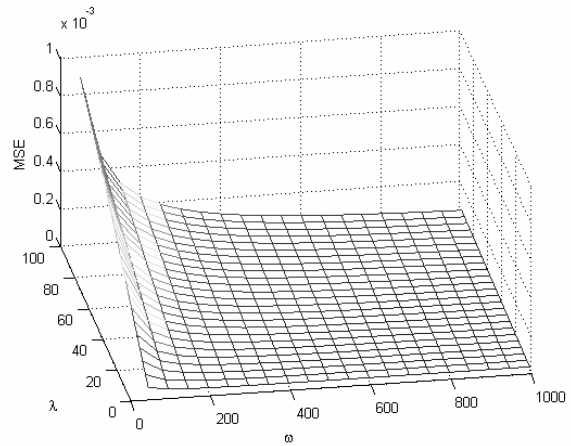


Figure 7. The MSE vs. ω and λ .

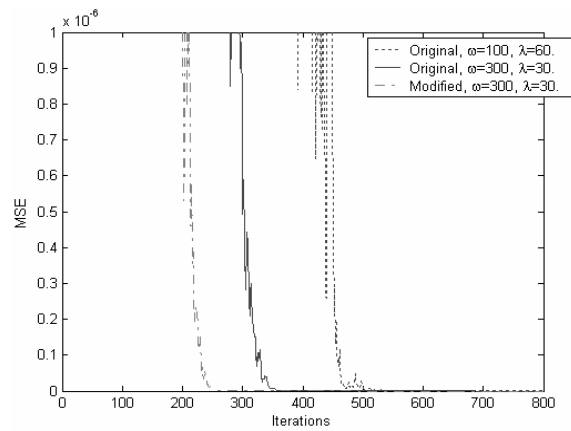


Figure 8. Rate of convergence of the conjugate gradient algorithm.

To complete the performance analysis of the proposed algorithm, we considered many different scenarios. In this paper, we present results that correspond to two of them: in the 1st scenario, a surface of small sample sizes is considered. A set of 52 sparse samples were randomly chosen from the reference surface. In the 2nd scenario, a surface of relatively medium sample sizes is considered. A set of 308 sparse samples were randomly chosen from the reference surface.

As expected, with a very small number of sparse patches, both the VSF and the MVSF algorithms performed better than the 3DHM algorithm. As it can be seen from Figure 9, the 3DHM cannot achieve an MSE of the ratio of 10^{-4} , while both other algorithms achieved such tolerance in less than 300 iterations.

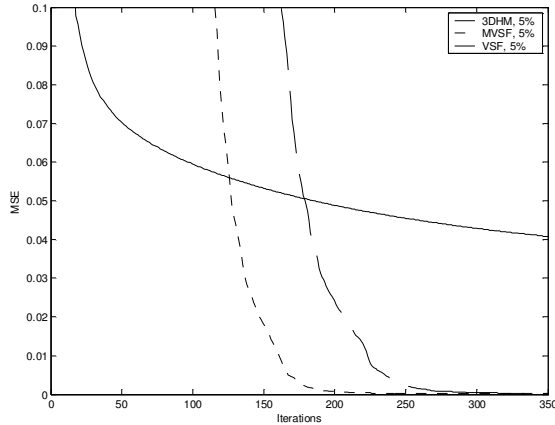


Figure 9. MSE comparison for the 1st scenario.

Figure 10 corresponds to the 2nd scenario, where about only 30% of the total mesh samples were chosen. In this case the 3DHM algorithm outperforms both the original and improved VSF algorithms. One may conclude that as the number of missing samples gets lower, it would be better using the 3DHM algorithm. In case of relatively small size of sparse data, it would be better using the MVSF algorithm. In general, the 3DHM algorithm is much faster than the two spline-based algorithms. For example, doing 300 iterations takes about 20 computation times longer for the original and modified algorithm than it takes for the 3DHM algorithm.

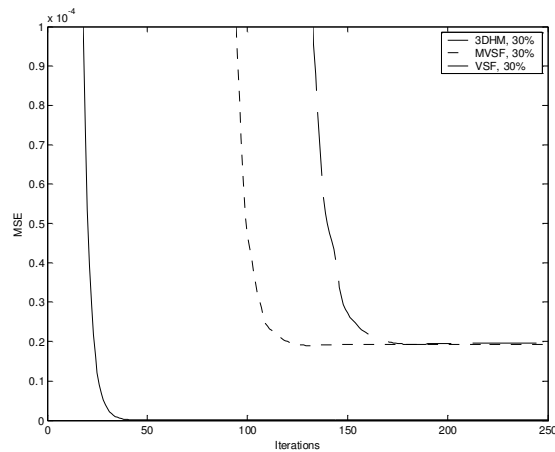


Figure 10. MSE comparison for the 2nd scenario.

4. 3D Surface Reconstruction Example

Smooth surface reconstruction techniques can be used for medical applications where relatively smooth organs like the left ventricle of the heart. In this section, the MVSF algorithm has been used to reconstruct the surface of the left ventricle of the heart starting with data acquired along three contours (Figure 11) extracted by a specialist from echocardiographic images. The 3D data is first transferred into a 2D developed surface (Figure 12). The available data is about 23% of the total mesh points. The missing points on the resulting incomplete surface are then estimated using the MVSF algorithm as shown in Figure 13. The reconstructed LV surface in Conclusion is a 3D representation of the 2D developed surface of Figure 13. Even if results from the original VSF algorithm looked visually similar, the computation time of the improved algorithm is relatively reduced. Using

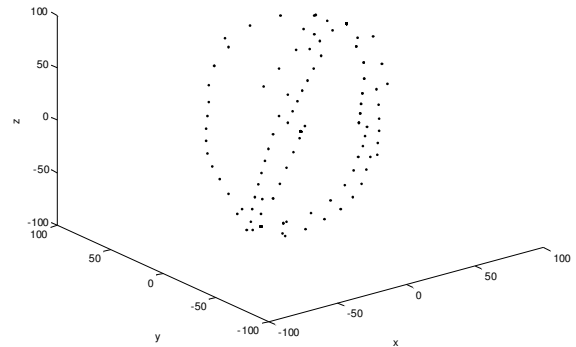


Figure 11. Three 3D contour data of a left ventricle.

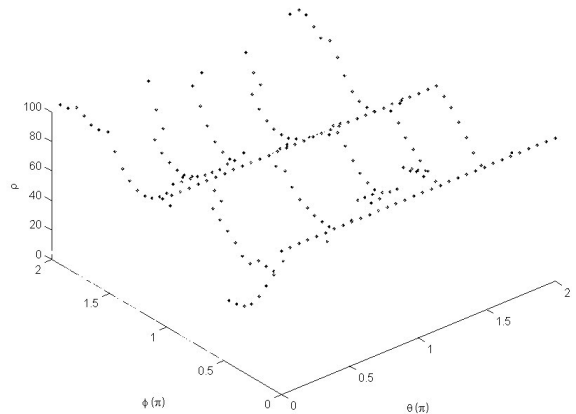


Figure 12. 2D developed incomplete surface of the left ventricle of Figure 11.

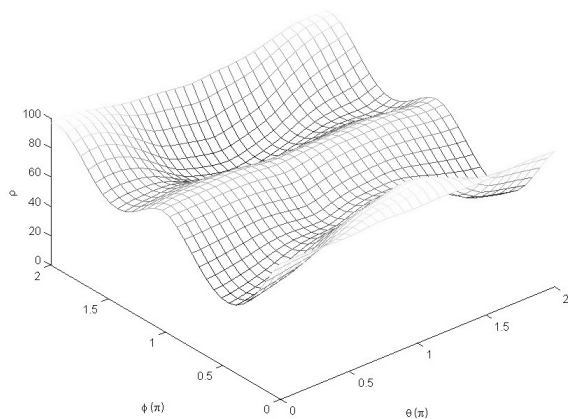


Figure 13. 2D developed surface from the original sparse data which are represented here by black dots.

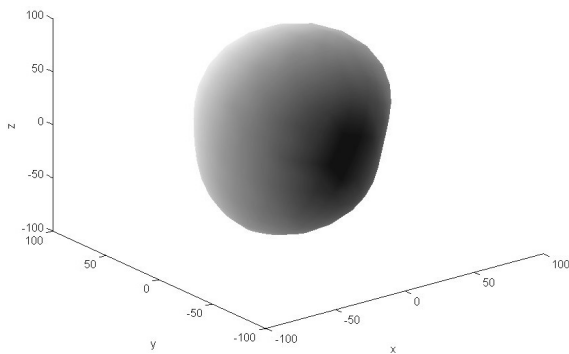


Figure 14. 3D reconstructed surface of the left ventricle using MVSF algorithm.

the same initial parameters to reconstruct the LV surface, the MVSF algorithm converges in about 50% faster than the original VSF algorithm, as a result of a reduction of about 100 iterations. As expected, the computation time of both VSF and MVSF is much higher when compared to the 3DHM algorithm.

5. Conclusion

In this paper, we presented an improved modification of the Variational Spline Fitting Algorithm. The proposed algorithm is based on a more accurate approximation of the energy equations in discrete time. Additionally, the algorithm takes into account the periodicity constraints which apply to our target application of modelling human internal organs such as the left ventricle of the heart. For simulated surfaces, we showed that our algorithm outperforms the original implementation discussed by Szeleski.

When compared to the 3DHM Fourier-based algorithm (developed earlier by the authors), the proposed algorithm was found to be best suited for the small sample-size case.

We have also shown that the proposed algorithm converges faster than the original one. Our results related to the reconstruction of the left ventricle of the heart have been very promising. We are currently investigating the use of the MVSF algorithm in 3D medical image registration.

References

- [1] O. GARCIA, A. SUSIN, Left ventricle's surface reconstruction and volume estimation. *Terceres jornades de recerca en Enginyeria Biomèdica*, (2002), Spain.
- [2] H. HOPPE, T. DEROSE, T. DUCHAMP, J. McDONALD, W. STUETZLE, Surface reconstruction from unorganized points. *The 19th Annual Conference on Computer Graphics and Interactive Techniques*, (1992).
- [3] S. GAO, H.-Q. LU, A Fast Algorithm for Delaunay based Surface Reconstruction. *The 11th International Conference in Central Europe on Computer Graphics, Visualization and Computer Vision*, (2003), China.
- [4] Y. F. WANG, J. F. WANG, Surface reconstruction using deformable models with interior and boundary constraints. *Journal of IEEE Transactions on Pattern Analysis and Machine Intelligence*, 14 (1992), pp. 572–579.
- [5] R. ENCISO, J. P. LEWIS, U. NEUMANN, J. MAH, 3D Tooth Shape from Radiographs using Thin-Plate Splines. *The 11th Annual Medicine Meets Virtual Reality Conference*, (2003), Newport Beach, California.
- [6] C. BONCIU, R. WEBER, C. LÉGER, 4D reconstruction of the left ventricle during a single heart beat from ultrasound imaging. *Journal of Image Vision Computing, Elsevier Eds*, 19 (2001), pp. 401–412.
- [7] R. SZELISKI, Fast surface interpolation using hierarchical basis functions. *Journal of IEEE Transactions on Pattern Analysis and Machine Intelligence*, 12 (1990), pp. 513–528.

Received: March, 2006

Accepted: April, 2007

Contact addresses:

Ahmad Almhdie
University of Orleans
12 rue de Blois
45067 Orleans Cedex 2
France

e-mail: ahmad.almhdie@univ-orleans.fr

Christophe Léger
 University of Orleans
 12 rue de Blois
 45067 Orleans Cedex 2
 France
 e-mail: christophe.leger@univ-orleans.fr

Maitine Bergounioux
 MAPMO, Faculté des Sciences
 Université d'Orléans
 France

Mohamed Deriche
 Electrical Engineering Department
 King Fahd University of Petroleum and Minerals
 Saudi Arabia

Roger Lédée
 LESI, Polytech'Orléans
 Université d'Orléans
 France

AHMAD ALMHDIÉ received the BSc degree in Electrical and Electronic Engineering from Al-Fateh University, Tripoli, Libya, in 1990, the MSc degree in Communication Engineering from McMaster University, Hamilton, Ontario, Canada, in 1999. His MSc research focused on the efficiency of the TDMA/SDMA frame generation process when using a switched parasitic antenna arrays for indoor smart antenna systems. From 1999-2002, he joined the department of Electrical and Communication Engineering at the University of Sebha, Sebha, Libya. He is currently a PhD student at Laboratory of Electronics, Signals, Images (LESI), University of Orléans, Orléans, France.

Almhdie's research interests include 3D image registration, surface reconstruction and local comparison of 3D medical data.

CHRISTOPHE LÉGER received the Ph.D. degree in Sciences for Engineering from the University of Orléans, France, in 1993. His research concerned the visualization of the volumic deformations of the left ventricle of the heart, using ultrasound images. This work was led in conjunction with the cardiology and nuclear medicine departments of the Hospital of Orléans. Since September 1998, he leads the LV4D (Left Ventricle of the heart in 4 Dimensions) team at the LESI (Laboratory of Electronics, Signals, Images).

Christophe Léger's primary research interests are spatio-temporal interpolation, Fourier analysis and dynamic modelling registration.

MAÏTINE BERGOUNIOUX is full Professor of Mathematics at the University of Orléans. Her research concerns mathematical and numerical analysis of partial derivative equation and particularly optimal command of systems. Bergounioux's research interests include image and signal processing, mathematical modeling and numerical analysis.

MOHAMED DERICHE received his B.S. degree from the National Polytechnic School of Algeria, Algiers, Algeria, and the M.S. and Ph.D. degrees from University of Minnesota, Minneapolis, in 1988 and 1992, respectively.

He taught at Queensland University of Technology, Australia, before joining King Fahd University of Petroleum and Minerals, Saudi Arabia, where he is currently leading the Signal Processing Group. He has published over 150 refereed papers. His research interests include multiscale signal processing, wavelets, fractals, with particular emphasis on multimedia applications and biometrics. Dr. Deriche has delivered numerous tutorial and invited lectures. He received the Best Electrical Engineering Student award at NPS and the IEEE Third Millennium Medal in 2000.

ROGER LÉDÉE received a Ph.D. Degree in Electronics from the University of Lille, France, in 1987. He joined the University of Orléans, France, since 1989 as a lecturer and researcher at LESI (Laboratory of Electronics, Signals, Images). His research concerned medical image processing for diagnostics purposes in nuclear medical imaging. He works in cooperation with the nuclear department of the hospital of Orléans.

Roger Lédée's research interests include registration, automatic segmentation, active contour models, shape recognition, cellular neural networks, deconvolution and quantification.
